Princeton Plasma Physics Laboratory

PPPL- 4702

PPPL- 4702

Observation of Global Alfven Eigenmode Avalanche Events on The National Spherical Torus Experiment

E.D. Fredrickson, N.N. Gorelenkov, E. Belova, N.A. Crocker, S. Kubota, G.J. Kramer, B. LeBlanc, R.E. Bell, M. Pedesta, H. Yuh and F. Levinton

November, 2011

PPPL PRINCETON PLASMA PHYSICS LABORATORY

Prepared for the U.S. Department of Energy under Contract DE-AC02-09CH11466.

Princeton Plasma Physics Laboratory
Report Disclaimers

Full Legal Disclaimer

Trademark Disclaimer

PPPL Report Availability

Princeton Plasma Physics Laboratory:

http://www.pppl.gov/techreports.cfm

Office of Scientific and Technical Information (OSTI):

http://www.osti.gov/bridge

Related Links:

U.S. Department of Energy

Office of Scientific and Technical Information

Fusion Links

Observation of Global Alfvén Eigenmode Avalanche events on the National Spherical Torus Experiment

E. D. Fredrickson, N. N. Gorelenkov, E. Belova, N. A. Crocker, S. Kubota, G. J. Kramer, B. LeBlanc, R. E. Bell, M. Podesta, H. Yuh, F. Levinton

1) Princeton Plasma Physics Laboratory, Princeton New Jersey 08543
2) Univ. of California, Los Angeles, CA 90095
3) Nova Photonics, Princeton, NJ 08543

email contact of main author: efredrickson@pppl.gov

Abstract. Instabilities excited by the fast-ion population on NSTX [M. Ono, *et al*., Nucl. Fusion **40** 557 (2000)] extend from low frequency Energetic Particle Modes (EPMs) at 10's of kHz, through Toroidal Alfvén Eigenmodes [TAE] in the range of 50kHz to 150kHz to Global and Compressional Alfvén Eigenmodes [GAE and CAE] in the frequency range of 0.3MHz to 2.5MHz, or roughly $0.1\omega_{ci}$ to $0.7\omega_{ci}$. The GAE instabilities exhibit complex non-linear behavior, including onset of strong growth above an amplitude threshold. This is conjectured to occur when resonance regions in phase space start to overlap, resulting in enhanced rapid growth and redistribution of energetic particles, a process referred to as an 'avalanche' [Berk, *et al*., Nucl. Fusion **35** (1995) 1661]. The GAE are suppressed following the avalanche, suggesting depletion of the fast ion population resonantly driving the modes, and in some instances the GAE bursts appear to trigger lower frequency TAE avalanches or Energetic Particle Modes, suggesting some significant redistribution of fast ions in phase space has occurred. These are the first observations of avalanching behavior for an instability driven through the Doppler-shifted cyclotron resonance. This paper also provides internal measurements of GAE mode structure showing that the mode amplitude peaks towards the plasma core.

I. INTRODUCTION

The National Spherical Torus Experiment (NSTX) [1] is a low aspect ratio (A = R/a ≈ 1.5) tokamak with maximum toroidal field of up to 5.5kG, plasma current of up to ≈1.2MA and neutral beam injection (NBI) heating of up to ≈ 6MW with 60kV to 90kV deuterium neutral beams. The relatively low magnetic field and high beam voltage result in a population of super-Alfvénic fast ions (ions with velocity greater than the Alfvén speed), much as is expected for many fusion reactor concepts where the fusion-generated α's will be super-Alfvénic. A wide range of instabilities excited by the fast ion population from neutral beam heating has been seen on NSTX [2-15], and other low aspect ratio tokamaks like MAST [16-22] and START [23,24].

Instabilities excited by the fast-ion population in NSTX extend from low frequency Energetic Particle Modes (EPMs) at 10's of kHz [25-28], through beta-induced Alfvén Acoustic Eigenmodes (BAAE) [29-31], Toroidal Alfvén Eigenmodes (TAE), 50 kHz to 150 kHz [2-11] up to Global and Compressional Alfvén Eigenmodes (GAE and CAE) in the frequency range of 0.3MHz to 2.5MHz, or roughly $0.1\omega_{ci}$ to $0.7\omega_{ci}$ [32-44]. Fast ion driven instabilities on NSTX can exhibit bursting, frequency chirping (up and/or down) and avalanching (a slow build-up in amplitude culminating in a final, rapid growth of one or more modes followed by a quiescent period [6,8,11, 45-47]).

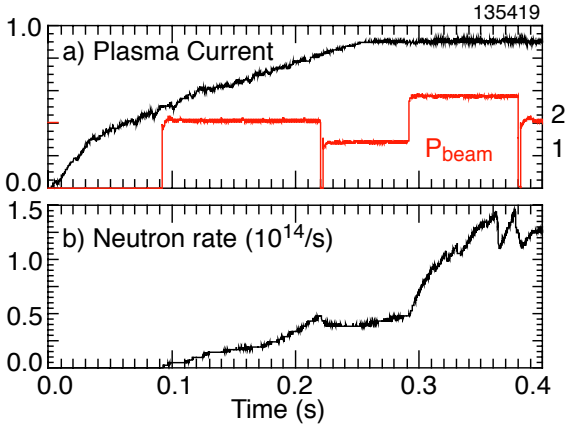

Fig. 1. a) Plasma current and heating beam power profile, b) neutron rate.

Global and Compressional Alfvén Eigenmodes are of interest for their possible roles in anomalous transport of fast ions, enhancement of electron thermal diffusivity [48,49], "alpha-channeling" [50-53], or stochastic heating of thermal ions [54-65]. The Doppler-shifted cyclotron resonance allows the modes to extract perpendicular energy from the fast ions, possibly enhancing fast-ion confinement. The trapped electron bounce frequency can be comparable to the GAE and CAE mode frequencies, resulting in the potential for resonantly-enhanced trapped-electron transport. Stochastic heating of the thermal ions by large amplitude, sub-cyclotron-frequency waves has been extensively investigated theoretically [54-59] and references therein] and experimentally [60-64], and proposed as method for direct thermal ion heating [65]. Above the amplitude for stochastic ion heating, the waves can very efficiently

transfer their energy to the thermal ion population, and the stochastic heating mechanism would tend to clamp the mode amplitude near the stochastic heating threshold. The avalanche mechanism can result in mode bursts with amplitudes much greater than the normal quasi-linear saturation amplitude, thus give the best chance for beam driven modes to exceed stochastic thresholds for thermal ion heating or trapped electron transport. Experimental measurements of the dynamics of mode amplitude and structure evolution are thus of interest.

GAE are seen in most NSTX beam heated plasmas, but GAE avalanches are less common. The plasma current, beam heating profile in time and neutron rate from a representative shot with GAE avalanches is shown in Fig. 1. The time history of beam voltage and power was optimized to excite TAE avalanches, and both TAE and GAE avalanching behavior is present. In this discharge, the GAE avalanches began around 0.23s and continued until ≈0.38s. The first TAE avalanche happened at ≈ 0.31s. The last, at ≈ 0.38s, triggered continuous n=1 activity. The avalanching activity may be suppressed after 0.38s due to an increase in density, the evolution of the q-profile, or redistribution of fast ions by the low frequency n=1 mode.

In the remainder of the paper, Sect. II will present measurements of the GAE mode, beginning with basic measurements of the mode wavelengths, internal structure and amplitude. The evidence for fast ion redistribution will be presented, followed by a discussion evidence for three-wave coupling of TAE and kinks, but not involving GAE. Section III will discuss the physics and issues relating to the resonant destabilization of the GAE and some implications of the observed mode amplitudes.

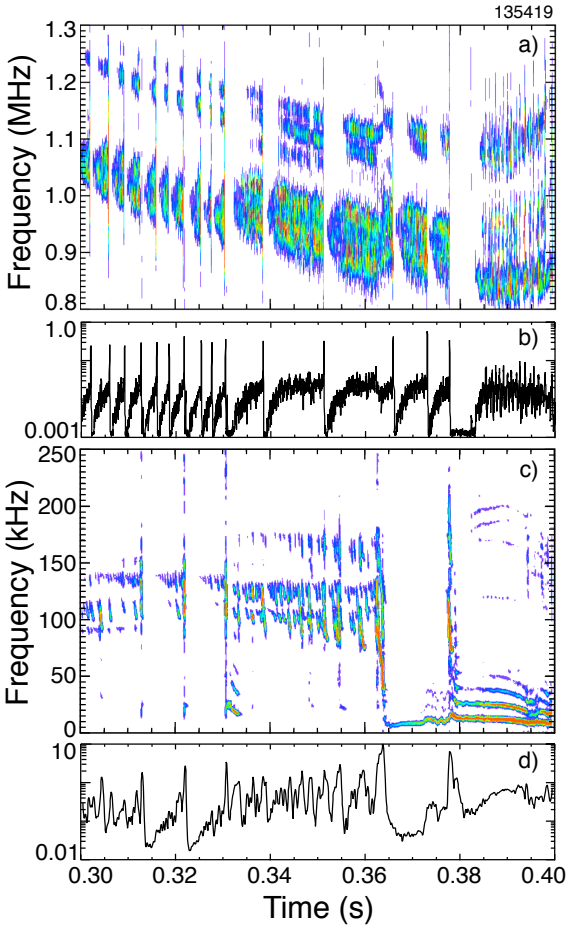

Fig. 2. a) spectrogram showing GAE modes, b) rms magnetic fluctuations 0.8MHz<freq<1.3MHz, c) spectrogram showing TAE and low frequency kink activity, d) rms magnetic fluctuations from 30kHz<freq< 200 kHz.

II. Experimental Observations

The diagnostics on NSTX with the bandwidth

and sensitivity to study modes in the MHz frequency range, for this shot, include the Mirnov coil arrays (for detection and measurement of poloidal and toroidal wavelengths) and the reflectometer arrays [66] (for measurement of the internal mode amplitude and radial structure). The reflectometers provide the only measurement of internal mode structure and amplitude for the experiments described here, but their use constrained the plasmas being studied to those with peaked density profiles (L-mode), ideally with a peak density on axis of a little more than ≈ 3.1 x $10^{19}/m^3$, the cut-off density of the highest frequency reflectometer channel at this time. For the 2010 campaign, a Beam Emission Spectroscopy (BES) diagnostic [67, 68] was added with requisite bandwidth and sensitivity to detect GAE modes, and the reflectometer array was upgraded to 16 channels with the density cut-off for the highest frequency channel extended to 7 x $10^{19}/m^3$.

GAE and TAE avalanches detected with a Mirnov coil are shown in Fig. 2. The spectrogram in Fig. 2a and rms fluctuation level in Fig. 2b show GAE avalanches in an L-mode plasma. Similarly, Figs. 2c and 2d show a spectrogram with five TAE avalanches, and the rms fluctuations in the TAE frequency band, respectively. The last TAE avalanche in these figures triggers a "saturated fishbone", that is, an n=1 kink mode that chirps down in frequency, but rather than decaying away, remains at nearly constant amplitude and frequency. These modes are likely the same as the "long-lived" modes reported on MAST [22,69].

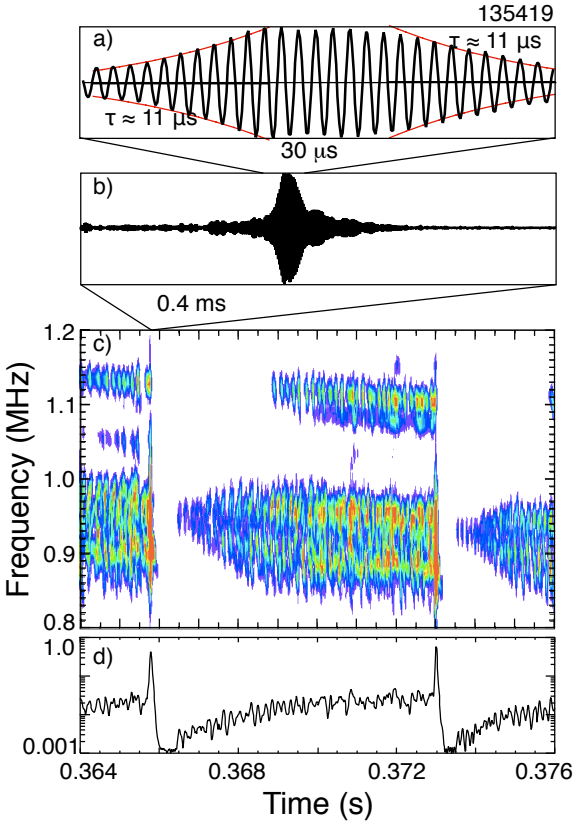

Fig. 3. a) final GAE avalanche burst measured with reflectometer with growth and decay rates of ≈ 0.9x10^5/s indicated, b) longer time period showing extended decay period, c) spectrogram over GAE avalanche cycle, rms amplitude evolution on semi-logarithmic scale.

The GAE avalanche period starts off short, about 3 ms, and then beginning after 0.33s lengthens to about 15 ms. The GAE amplitude increases exponentially for several milliseconds after each avalanche (that is a linear increase in the semi-logarithmic plot, Fig. 2b), reaching nearly the same amplitude in each of the avalanche periods before the rapid growth of the final burst is

triggered. This two-stage growth process provides strong evidence of avalanche behavior. In the later, longer avalanche periods, the mode amplitude nearly saturates at a level below the apparent threshold for rapid growth. There is a period of saturation or much slower growth following the initial linear growth leading up to the rapid growth, or avalanche, phase. The peak amplitude of the final avalanche bursts, which appear as spikes in the rms plot (Fig. 2b), is relatively constant for the 15 avalanches seen in Figs. 2a and 2b.

The spectrogram in Fig. 3c shows one of the later GAE avalanche cycles from ≈ 0.366s to ≈ 0.373s. The pre-avalanche fluctuations are seen to be an almost turbulent spectrum of fluctuations in a frequency band about 100 kHz to 150 kHz wide. These fluctuations are a mix of toroidal mode numbers, ranging from n = 7 to n = 11 (all counter propagating to the neutral beams). The rms fluctuation amplitude is shown in Fig. 3d on a semi-logarithmic scale. The GAE amplitude nearly saturates before the final order of magnitude jump in mode amplitude at the end of the avalanche cycle. In Fig. 3b is shown a trace of the phase fluctuations from a quadrature reflectometer signal showing the final, large burst, which is further expanded in Fig. 3a, where growth and decay times of ≈ 11 μs are seen. The final large burst consists of only several 10's of wave cycles near the peak amplitude.

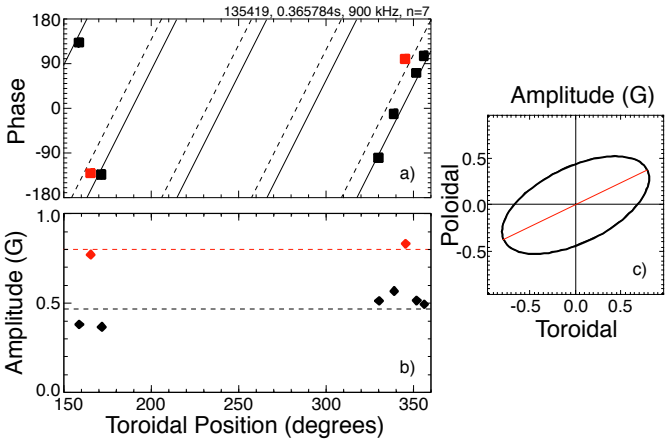

Fig. 4. a) Relative phase data from Mirnov coil array. Red points are toroidally-oriented coils, black poloidal, b) fluctuation amplitude in Gauss, c) composite Lissajous figure based on amplitude and phase data.

IIa Structure of GAE

The toroidal mode number and polarization of the magnetic fluctuations are measured with a toroidal array of eight Mirnov coils, six oriented to measure the poloidal component and two oriented to measure the toroidal component of the magnetic fluctuations (Fig. 4). As an example, the best fit to the toroidal mode number of the dominant spectral peak of the magnetic fluctuations in the final burst in a later avalanche (0.366s) is n = 7 (as it is in the other avalanches). However, decomposing the signal into the n='odd' and n='even' components demonstrates that there is a significant even component to the mode, and an additional n=7±2

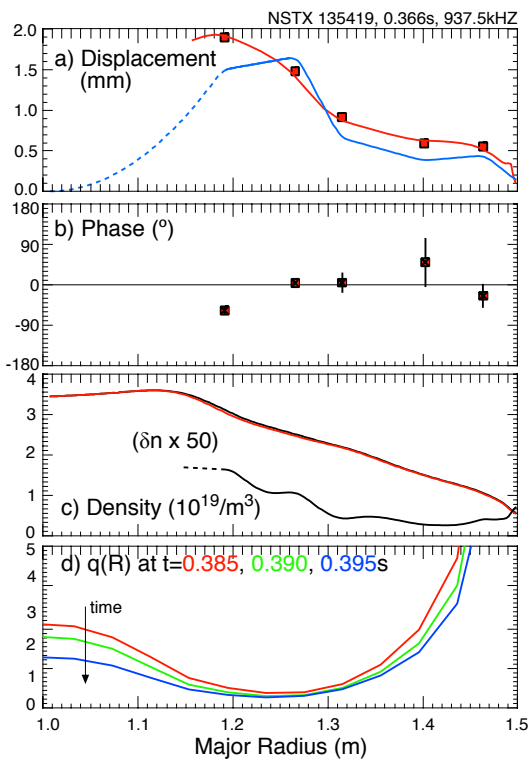

Fig. 5. a) Mode amplitude profile from reflectometer array, b) relative phase of mode, c) density profile, d) q-profile from equilibrium reconstruction with MSE pitch-angle data.

component may be inferred from the amplitude modulation of the n='odd' component. The mode is mostly compressional at the plasma edge; the dominant magnetic perturbation is larger parallel to the equilibrium magnetic field than in the transverse direction.

The amplitude evolution and radial profile are measured with a five-channel reflectometer system. The displacement profile obtained from the reflectometer array data is shown in Fig. 5a. The red squares are the phase fluctuation amplitudes from the quadrature reflectometer channels, converted by the free-space wavelength to an effective displacement in mm. The blue curve, Fig. 5a, is the effective displacement of the equilibrium density profile (that is assuming shear polarization for the wave with no compressional terms) needed to reproduce the observed reflectometer data (red curve, Fig. 5a). The solid black curve, Fig. 5c, is the density perturbation, correcting for interferometric contributions, inferred from the reflectometer data, independent of the shear or compressional nature of the wave. The inferred density perturbation is multiplied by 50 (solid black curve) to be visible in this figure, and the peak perturbed density is $\delta n/n \approx 1\%$. The relative phases of the density fluctuations measured by the five channels are shown in Fig. 5b. The q-profiles deduced from equilibrium reconstructions constrained with MSE data, starting 20 ms after the GAE burst when MSE data becomes available, are shown in Fig. 5d. The mode amplitude appears to peak near or inside of q_{min}.

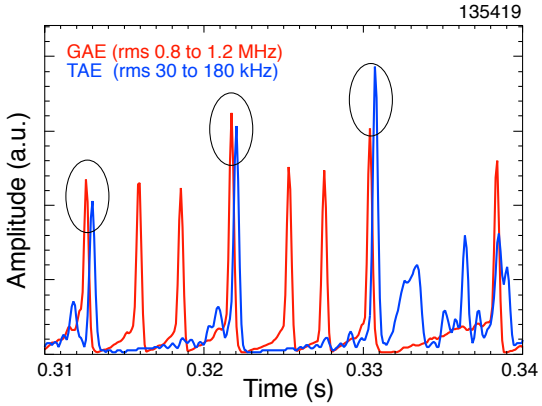

Fig. 6. RMS fluctuation levels in GAE frequency band (red) and TAE frequency band (blue). Relative fluctuation amplitudes between red/blue curves is arbitrary; shown for timing only.

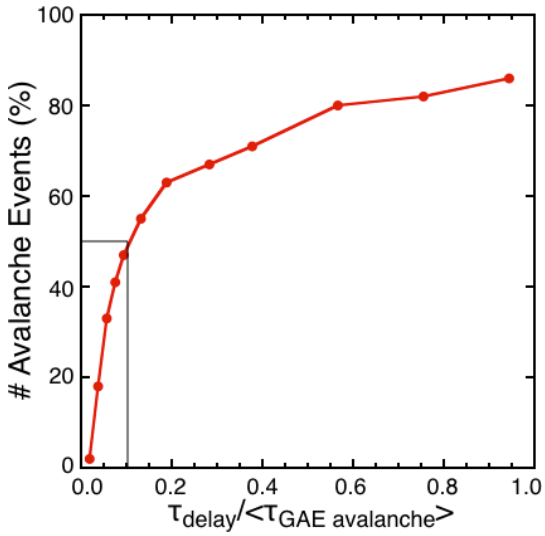

Fig. 7. Percent of TAE avalanche events occurring in the time interval following a GAE avalanche, normalized to the average TAE avalanche period.

IIb GAE induced fast ion transport

Neutron rate drops, or evidence of fast ion redistribution or loss in the Fast Ion D-Alpha (FIDA) [70] or scintillator Fast Lost Ion Probe (sFLIP) [71] data, are not seen to correlate with the GAE avalanches. Indeed, as will be discussed later, the interaction of the resonant fast ions exciting these modes may actually improve their confinement. However, the GAE-quiescent period following each strong burst is consistent with a fast-ion redistribution which reduces the free-energy available to drive the modes. Additional indirect evidence of fast ion redistribution is shown in Fig. 6, where the rms fluctuation level for GAE (red) and TAE (blue) are shown. The three TAE avalanche events in this time range, at 0.313s, 0.322s, and 0.331s, are seen as spikes in the blue curve. A GAE avalanche precedes each of the three TAE avalanches by several hundred microseconds, although not every GAE avalanche is followed by a corresponding TAE avalanche. The timing suggests that the redistribution of fast ions from the GAE avalanche provided some of the impetus to trigger the TAE avalanche.

A database was compiled of the timing of 358 GAE avalanches and 51 TAE avalanches in shots where GAE and TAE avalanches co-existed. In Fig. 7 it is seen that 50% of the TAE avalanches occur within the first 10% of the GAE avalanche cycle. If the timing of the TAE avalanches were not correlated with the GAE avalanches, the curve would be approximately linear, with ≈10% of the TAE avalanches in the first 10% of the GAE avalanche cycle. The occurrence of the TAE avalanches shortly after the GAE avalanche suggests a causal relation.

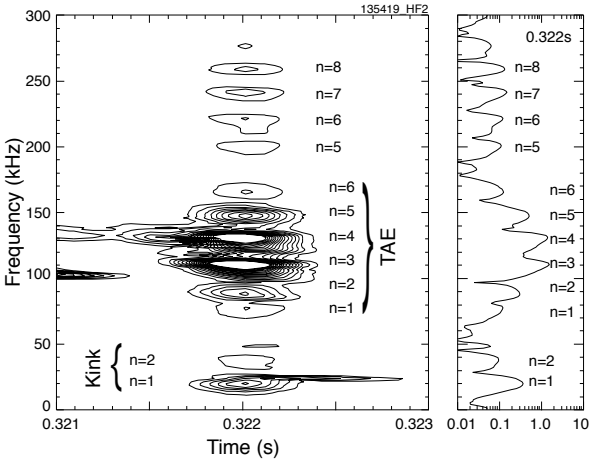

Fig. 8. Spectrogram of Mirnov coil signal showing a) multiple modes with toroidal mode numbers identified, b) spectrum at 0.322s on logarithmic scale.

IIc Three-wave coupling in TAE, not GAE

The correlation of the TAE and GAE avalanches is most likely to occur through changes to the fast ion distribution, however, three-wave coupling of TAE to a much lower frequency kink (and higher frequency modes) has been previously observed on NSTX [72]. As is seen below, there is no apparent wave-wave coupling of the GAE and TAE, leaving modifications to the fast ion distribution as the most likely candidate for the triggering of the TAE avalanches by the GAE.

A spectrogram of the TAE avalanche at 0.322s is shown in Fig. 8. There are n = 1 through n = 6 TAE in the final TAE avalanche burst, with the two dominant modes being the n = 3 and n = 4. The modes are approximately evenly spaced in frequency, within the ±3 kHz accuracy resulting from the short, ≈ 0.2 ms, period of the final TAE avalanche burst. A second group of modes in a frequency band 180kHz to 300kHz have mode numbers and frequencies which satisfy the non-linear mode coupling relations that $f_3 = f_1+f_2$ and $n_3 = n_1+n_2$ for the TAE modes in the frequency range 70 kHz to 180 kHz. For example, the frequency of the n = 7 mode at 240 kHz is, within measurement accuracy, the sum of either of the n = 3 and n = 4, the n = 2 and n = 5 or the n = 1 and n = 6 mode frequencies. Similarly, the n=1 mode at ≈ 20 kHz is consistent with the difference frequency of the n = 4 and n = 3 modes [72].

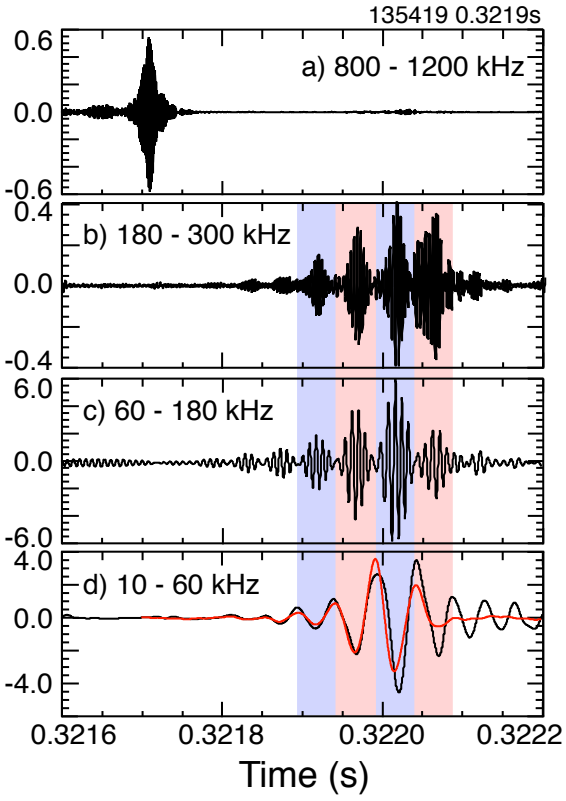

Fig. 9. Mirnov coil digitally bandpass filtered in three ranges showing a) GAE burst, b) TAE frequency doubling, c) TAE avalanche and d) n=1 internal kink, red curve is a simulation of non-linear coupling, scaled to match the kink.

The Mirnov signal through the GAE and TAE bursts is shown in more detail in Fig. 9. The Mirnov coil signal is digitally filtered into four frequency bands. The GAE avalanche burst is seen in the frequency band from 0.8 MHz to 1.2 MHz (Fig. 9a) and the TAE avalanche burst in the range from 60 kHz to 180 kHz (Fig. 9c). It's clear that the GAE burst precedes the onset of the TAE avalanche. The amplitude modulation of the TAE-frequency fluctuations is due to the

beating of the dominant, nearly equal amplitude n = 3 and n = 4 modes. Figs. 9b and 9d show the digitally filtered signal for the frequency bands covering the sum and difference frequencies of the TAE modes.

The non-linear coupling of the low and high frequency bursts can be simulated by squaring the bandpass filtered TAE fluctuations (Fig. 9c), and again filtering the result to separate the 20 kHz component. This is shown in Fig. 9d where the red curve is the simulated non-linear coupling, inverted and scaled to match the measured n = 1 mode amplitude [72]. The simulated and experimental signals initially track well, but later diverge, suggesting that an independent n = 1 mode was excited at the difference frequency, which then decayed when the non-linear drive from the TAE burst was gone.

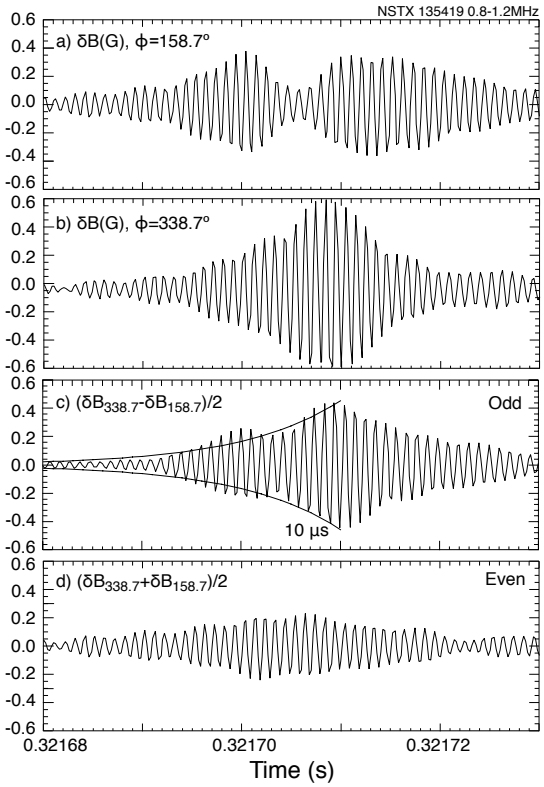

Fig. 10. a) digitally filtered Mirnov coil signal from toroidal angle of 171.5°, b) similar from 351.5°, c) Odd component of final GAE avalanche burst with growth rates of 10^5/s and $2x10^5$/s indicated, d) even component (from Mirnov coils).

In Fig. 10 the GAE burst of Fig. 8a is shown on an expanded timescale. Here the magnetic fluctuations as measured with two coils separated by 180° in the toroidal direction (Figs. 10a and 10b) are separated into the odd-n and even-n components (Figs. 10c and 10d). The odd component still shows evidence of beating in the amplitude evolution, consistent with an additional odd toroidal mode of smaller amplitude. The even component is somewhat weaker, also with possibly some weak beating. The difference frequency is about 100 kHz, as estimated by the beat period in Figs. 10c and 10d. This is roughly equal to the TAE frequency, but apparently is not a non-linear 3-wave coupling with the TAE as the TAE amplitude is small at this time (Figs. 9a and 9c). Further, the mode number difference for the GAE is 1 or 2, whereas the dominant TAE activity is n = 3 and n = 4. Thus, it appears that the GAE avalanche burst does not exhibit strong non-linear coupling to the TAE, but rather involves two or more nearly independent modes.

III. Discussion and analysis

These observations of GAE activity are relevant to the physics of fast-ion avalanches, stochastic ion heating, alpha-channeling, and fast ion redistribution. In this section, the measurements of mode structure and mode amplitude evolutions are examined with respect to these various areas of fast particle driven mode physics. But first, the identification of the modes and the resonant drive for the modes is discussed.

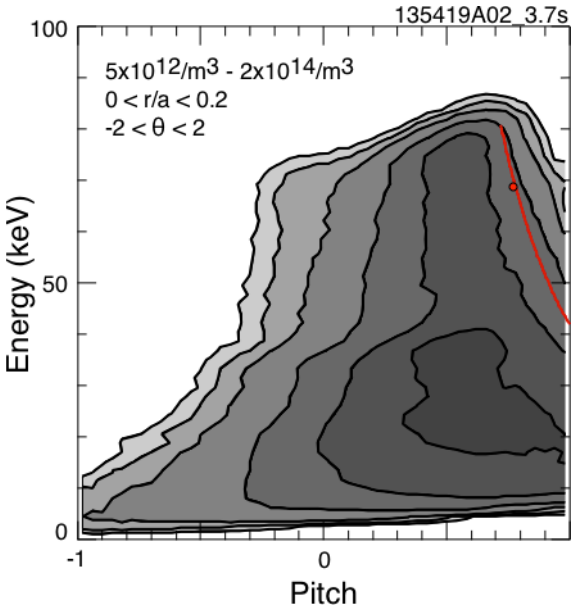

Fig. 11. Distribution function calculated with the TRANSP beam deposition code. Red curve indicates fast ions resonant with dominant n = 9 mode. The red point indicates pitch and energy of particle whose trajectory is shown in Fig. 12.

The profile of the internal density fluctuation is measured with the reflectometer array, and the magnetic fluctuations are measured externally with Mirnov coils. There are no reflectometer measurements for R < 1.2m, but this data indicates that the density fluctuations peak near or inside the region of q_{min}. This would be consistent with identification of these modes as GAE, rather than CAE, which should have had a peak in amplitude further out. The pitch of the magnetic field perturbation measured at the plasma wall indicates that the mode has some compressional component, whereas GAE are in principal shear Alfvén waves. However, toroidicity, magnetic shear and finite beta are observed to introduce compressional components in numerical simulations of GAE for NSTX parameters [43], thus edge polarization measurements are inconclusive regarding mode identification.

The pitch of fast ions resonant with the mode can be estimated from the local GAE dispersion relation $\omega = k_{||} V_{Alfvén}$ and the Doppler-shifted cyclotron resonance condition, $\omega = \omega_{ci} - k_{||}V_{b||}$. The GAE dispersion relation is used to estimate $k_{||}$ from the mode frequency in the plasma frame and the local Alfvén velocity. The resonant pitch is then $V_{b||}/V_b = (\omega_{ci} - \omega)/\omega (V_{Alfvén}/V_b)$. For the dominant n = 9 mode in the avalanche burst, this gives a pitch of $V_{b||}/V_b \approx 0.7$ for the resonant 80 keV fast ions. As the ion energy drops, the pitch required for

resonance increases, that is the parallel energy remains constant to satisfy the resonance condition, but the perpendicular energy can be lower, resulting in higher pitch.

The fast ion distribution function calculated in TRANSP is shown in Fig. 11 and the resonant condition as a function of energy, constant parallel velocity, is indicated by the red line. The resonance curve sits on the side of a 'bump-on-tail' in perpendicular energy, but a more comprehensive analysis of the stability and resonant drive physics are beyond the scope of this paper. Numerical simulations have been done [43] and an analytic model of the Doppler-shifted cyclotron resonance instability has been developed [73].

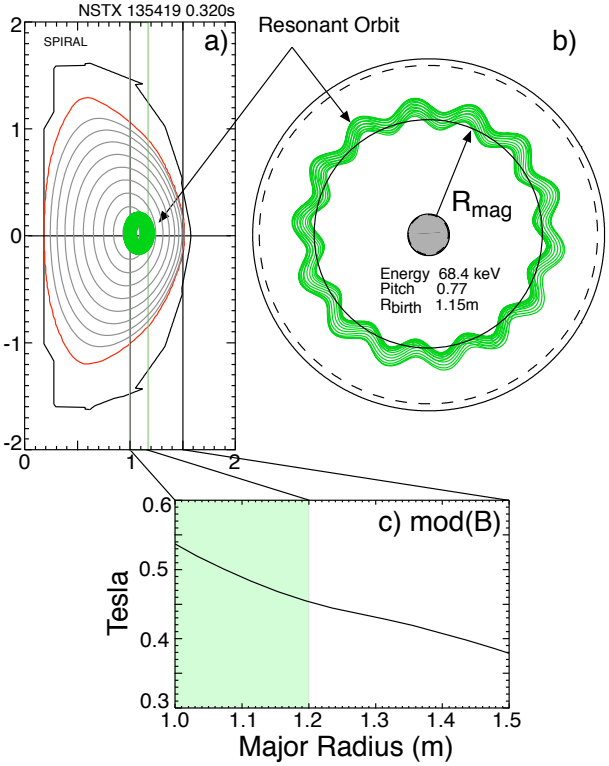

Fig. 12. Orbit of a representative fast ion resonant with the GAE, a) mapped to the poloidal cross-section, b) plan view and c) mod(B) on midplane with shaded region showing the range of the guiding center.

One challenge for analytic models of the Doppler-shifted cyclotron resonance in low aspect ratio plasmas is that the orbits of most fast ions move over a wide range of magnetic field strengths, and thus the cyclotron frequency changes significantly over the orbit. As the resonance with the mode, $\omega_{ci}-k_{||}V_{b||}=\omega_{mode}$, depends on the cyclotron frequency, fast ions will move into and out of resonance on a timescale short compared to a wave period. However, a numerical simulation of GAE with the initial value code, HYM, has been able to demonstrate instability of both GAE and CAE through the Doppler-shifted cyclotron resonance drive. The typical fast ions resonant with the GAE in the HYM simulation have passing orbits constrained to the outboard midplane. An example orbit calculated with the SPIRAL [74] code is mapped to a poloidal cross-section as shown in Fig. 12. The radial extent of the orbit guiding center corresponds to a variation in cyclotron frequency of only ±5%, or a frequency modulation amplitude of ≈200 kHz (out of $\langle f_{ci} \rangle \approx 3.9$ MHz). There are approximately 16 gyro-periods in each poloidal transit, or $f_{pol} \approx 3.9$ MHz/16 ≈ 245 kHz. In the resonant fast ion frame, the mode frequency is Doppler-shifted to match the cyclotron

frequency, as noted previously ($\omega + k_{||}V_{b||} = \omega_{ci}$). The relative phase variation between the mode and the cyclotron gyrations over a poloidal transit can be estimated by integrating the approximate modulation of the cyclotron frequency and parallel velocity. The approximate formula for the phase variation is

$$\delta\phi(t) \approx \frac{< k_{\|}V_{B\|} >}{\omega_T}\frac{\varepsilon}{2}\frac{1-p^2}{p^2}\sin(\omega_T t) + \frac{< \omega_{ci} >}{\omega_T}\varepsilon\sin(\omega_T t)$$

For the fast ion parameters shown in Fig. 12, the amplitude of the phase modulation over a poloidal transit is ≈ 65º; probably large enough to affect the mode drive and the fast ion trapping, but probably not large enough to destroy the resonance.

The early GAE amplitude evolution is suggestive of avalanching behavior, with a slow growth in mode amplitude as the fast ion population builds up, leading to a short, explosive growth to much larger amplitude which is then followed by a quiescent period. After 0.33s, however, the slow growth seems to saturate for an extensive period of time. This could be explained if the mode amplitude saturated just below the threshold for triggering an avalanche. An intriguing alternative explanation is that this represents the "stochastic thermal ion heating" threshold. At this amplitude, there is an effective damping term increasing strongly with mode amplitude as the wave dumps energy into the thermal ion population. In the 'linear' regime, the mode drive is fixed or falling with mode amplitude and this quickly leads to saturation. The potential effective heating power is estimated below, but depending upon how far below the 'natural' saturation amplitude the stochastic threshold is, a still substantial portion of the power will go to the electrons through Landau damping.

The presence of multiple modes in the final, large bursts, is indicated by the amplitude modulations of the even and odd signals. The presence of the multiple modes complicates the measurement of the growth and damping rates in the final burst. However, the observed growth and decay of the final bursts appears roughly symmetrical, with growth and damping times of approximately 10 μs, or $\gamma/\omega \approx 3.4\%$. If the assumption is made that the drive is negligible during

the burst decay, Fig. 4a suggests that the peak drive, γ_{drive} is approximately twice the damping rate, γ_{damp}, *e.g.*, $\gamma_{growth} = \gamma_{drive} - \gamma_{damp} \approx \gamma_{damp} \approx 10^5/s$.

The peak mode amplitude of $\delta n/n \approx 1\%$ can be used to estimate the magnetic fluctuation level, which together with the growth/damping rate estimate can be used to estimate the power flow from the fast ion population through the mode and into the thermal plasma. For compressional modes, the relation is $\delta B/B \approx \delta n/n$, for shear modes, the relation is more complicated, but roughly $\delta B/B \approx L_n/L_B\ \delta n/n$, where L_B is the relevant magnetic gradient scale length. As the magnetic gradient scale length is typically greater than the density gradient scale length, the magnetic perturbations for shear waves would generally be weaker, for a given density perturbation, than for compressional waves. In the following discussion, we use the larger estimate for magnetic fluctuations from the compressional approximation to give an upper estimate for energy in the mode. The peak amplitude of $\delta n/n \approx 1\%$ implies $\delta B/B \leq 1\%$ or $\delta B \approx 40$G.

The total energy density in the wave may be estimated as twice $4\text{x}10^{-3}$ J/m^{3}G^2 (40 G)$^2 \approx 13$ J/m^3. The wave amplitude is small outside of $R \approx 1.3$m, thus the plasma volume where mode amplitude is significant is ≈ 3.2 m^3, and the peak wave stored energy is ≈ 40 J. These estimates are very approximate, but suggest that ≈ 40 J of energy is transferred from the fast ion population to the thermal plasma at each GAE avalanche event. The ten avalanche events between 0.3 and 0.33s give an average heating power of ≈ 13 kW. The peak heating power from the pre-avalanche phase, assuming an effective damping rate of 10^5/s, and roughly 10% of the amplitude reached during the avalanche, is ≈ 50kW, although the time average would be much less. Much of this power, of course, goes to the electrons through electron Landau damping.

The estimated peak density fluctuation level reaches $\delta n/n$ of approximately 1%; a level which might exceed the threshold for stochastic heating of thermal ions or transport of trapped electrons. Simulations of thermal ion heating were performed with a fixed spectrum of 20 modes, each with amplitude of $\delta B/B \approx 0.13$ %, or $20^{1/2}\delta B/B \approx 0.6$ %, gave heating rates of up to 50 eV/ms in perpendicular energy, and 17 eV/ms in parallel energy [75]. The estimated peak GAE amplitude of $\delta B_{rms}/B \approx 1$ % during the avalanche burst is comparable, albeit comprised of an unknown number of modes. The heating rate increases non-linearly with mode amplitude,

but the typical burst duration of ≈ 20 μs would result in a thermal temperature rise of < 1 eV per GAE avalanche. Using the same formalism as above with an ion density of $2.4 \times 10^{19}/m^3$, predicts a net increment to the ion thermal energy of ≈ 4 J, compared to the estimate of 40 J of heating made above. The thermal ion heating at the pre-avalanche level of 10 % of the avalanche peak amplitude, or 0.02 %, is predicted to result in negligible heating of the thermal ions. Stochastic ion heating may play a role in limiting the peak amplitude of the avalanche, but appears to play a negligible role in the thermal ion power balance.

A broad spectrum of GAE activity has also been implicated in enhanced electron thermal transport [48], most often correlated with a flattening of the electron temperature profile in the core. Such flattening is associated with density fluctuation amplitudes of $\delta n/n \approx 0.1\%$, which is comparable to the pre-avalanche level, and much less than the peak amplitude of $\delta n/n \approx 1$ %. Whether this interaction with the thermal electrons can provide some additional drive for the GAE, and how this affects the avalanche model, will be the object of further research.

IV. Summary

A broad spectrum of modes in the frequency range from 0.5 MHz to 1.5 MHz is often seen in NSTX beam heat plasmas. The modes are surmised to be Global Alfvén Eigenmodes based on their spectrum and evolution of frequencies. The GAE are expected to be localized near the low shear region of minimum q. Internal measurements show modes are indeed peaked toward the magnetic axis, possibly near the off-axis minimum in q. The peak mode amplitude as measured with the reflectometers reaches $\delta n/n \approx 1\%$. The modes exhibit a range of behavior, including chirping, bursting as well as more continuous activity. In this paper we have presented data documenting behavior characterized as avalanching, a slow growth in mode amplitude following a quiescent period, culminating in very rapid growth of multiple modes leading again to a quiescent period. The avalanches are seen to involve multiple modes with toroidal mode numbers from roughly n = 7 to n = 11.

The modes are postulated to be excited through a Doppler-shifted cyclotron resonance with beam ions, an assumption supported by numerical simulations. We have estimated the energy dependence on pitch-angle for fast ions satisfying this resonance condition and have shown that it aligns well with the distribution of fast ions calculated with the TRANSP code. We deduce that

these avalanches redistribute fast ions from the quiescent period following the avalanche burst and by the apparent triggering of TAE mode avalanches at lower frequency. So far, direct measurements of fast ion population have been insufficiently sensitive to detect this implied redistribution. However, it is quite possible that the fast ion redistribution results in improved confinement, as the cyclotron resonance should increase the pitch of fast ions, making their velocities more parallel and generally better confined.

BIBLIOGRAPHY

[1] M. Ono, S.M. Kaye, Y.-K.M. Peng, G. Barnes, W. Blanchard, M.D. Carter, J. Chrzanowski, L. Dudek, R. Ewig, D. Gates, R.E. Hatcher, T. Jarboe, S.C. Jardin, D. Johnson, R. Kaita, M. Kalish, C.E. Kessel, H.W. Kugel, R. Maingi, R. Majeski, J. Manickam, B. McCormack, J. Menard, D. Mueller, B.A. Nelson, B.E. Nelson, C. Neumeyer, G. Oliaro, F. Paoletti, R. Parsells, E. Perry, N. Pomphrey, S. Ramakrishnan, R. Raman, G. Rewoldt, J. Robinson, A.L. Roquemore, P. Ryan, S. Sabbagh, D. Swain, E.J. Synakowski, M. Viola, M. Williams, J.R. Wilson and the NSTX Team, Nucl. Fusion 40 (2000) 557.

[2] N N Gorelenkov, C Z Cheng, G Y Fu, S Kaye, and R White, Phys. of Plasmas **7** (2000) 1433.

[3] E.D. Fredrickson, C.Z. Cheng, D. Darrow, G. Fu, N.N. Gorelenkov, G Kramer, S S Medley, J. Menard, L. Roquemore, D. Stutman[1], R. B. White, Phys. of Plasmas **10** (2003) 2852.

[4] W W Heidbrink, E Fredrickson, N N Gorelenkov, A W Hyatt, G Kramer and Y Luo, Plasma Physics and Controlled Fusion **45** (2003) 983.

[5] E.D. Fredrickson, R. Bell, D. Darrow, G. Fu, N. Gorelenkov, B. LeBlanc, S. Medley, J. Menard, H. Park, L. Roquemore, S. A. Sabbagh, D. Stutman, K. Tritz, N. Crocker, S. Kubota, W. Peebles, K.C. Lee, F. Levinton, Phys. of Plasmas **13** (2006) p056109.

[6] E.D. Fredrickson, N N Gorelenkov, R E Bell, J E Menard, A L Roquemore, S. Kubota, N A Crocker, W Peebles, Nucl. Fusion **46** (2006) s926.

[7] N. A. Crocker,W. A. Peebles, S. Kubota, E. D. Fredrickson, S. M. Kaye, B. P. LeBlanc, J. E. Menard, Phys. Rev. Lett. **97** (2006) 045002.

[8] M. Podestà, W. W. Heidbrink, D. Liu, E. Ruskov, R. E. Bell, D. S. Darrow, E. D. Fredrickson, N. N. Gorelenkov, G. J. Kramer, B. P. LeBlanc, S. S. Medley, A. L. Roquemore, N. A. Crocker, S. Kubota, and H. Yuh, Phys. Plasmas **16** (2009) 056104.

[9] W W Heidbrink, E Ruskov, E D Fredrickson, N Gorelenkov, S S Medley, H L Berk and R W Harvey, Plasma Phys. Control. Fusion **48** September 2006) 1347-1372

[10] E.D. Fredrickson, R. Bell, D. Darrow, G. Fu, N. Gorelenkov, B. LeBlanc, S. Medley, J. Menard, H. Park, L. Roquemore, S. A. Sabbagh, D. Stutman, K. Tritz, N. Crocker, S. Kubota, W. Peebles, K.C. Lee, F. Levinton, Phys. of Plasmas **13** (2006) p056109.

[11] E. D. Fredrickson, N. A. Crocker, R. E. Bell, D. S. Darrow, N. N. Gorelenkov, G. J. Kramer, S. Kubota, F. M. Levinton, D. Liu, S. S. Medley, M. Podestá, K. Tritz, R. B. White, and H. Yuh Phys. of Plasmas **16** (2009), 122505.

[12] E. D. Fredrickson, N. N. Gorelenkov and J. Menard, Phys. of Plasmas 11 (2004) 3653.

[13] E D Fredrickson, C Z Cheng, L Chen, D Darrow, N N Gorelenkov, D Johnson, S Kaye, S Kubota, J Menard, R B White, Proc.of 29th EPS Conf. on Plasma Physics and Controlled Fusion, Montreaux, 17-21 June 2002 ECA Vol. **26B**, paper P-1.104 (2002)

[14] H. L. Berk, C. J. Boswell, D. Borba , B. N. Breizman, A. C. A. Figueiredo, E. D. Fredrickson, N. N. Gorelenkov, R. W. Harvey, W. W. Heidbrink, T. Johnson, S. S. Medley, M. F. F. Nave, S. D. Pinches, E. Ruskov, S. E. Sharapov, and JET EFDA contributors, in proceedings of the 21st IAEA Fusion Energy Conference. 16 - 21 October 2006, Chengdu, China (IAEA, Vienna, 2007) paper IAEA-TH/3-1

[15] E D Fredrickson, N N Gorelenkov, C Z Cheng, R. Bell, D. Darrow, D. Gates, D. Johnson, S. Kaye, B. LeBlanc, D. McCune, J. Menard, S. Kubota, W. Peebles, Phys. of Plasmas **9** (2002) 2069.

[16] Sharapov, S.E., Alper, B., Andersson, F., Baranov, Yu.F., Berk, H.L., Bertalot, L., Borba, D., Boswell, C., Breizman, B.N., Buttery, R., Challis, C.D., de Baar, M., de Vries, P., Eriksson, L.-G., Fasoli, A., Galvao, R., Goloborod'ko, V., Gryaznevich, M.P., Hastie, R.J., Hawkes, N.C., Helander, P., Kiptily, V.G., Kramer, G.J., Lomas, P.J., Mailloux, J., Mantsinen, M.J., Martin, R., Nabais, F., Nave, M.F., Nazikian, R., Noterdaeme, J.-M., Pekker, M.S., Pinches, S.D., Pinfold, T., Popovichev, S.V., Sandquist, P., Stork, D., Testa, D., Tuccillo, A., Voitsekhovich, I., Yavorskij, V., Young, N.P., Zonca, F., Nuclear Fusion Sept. 2005, Vol. 45, no.9, pp. 1168-77.

[17] A Sykes, R J Akers, L C Appel, E R Arends, P G Carolan, N J Conway, G F Counsell, G Cunningham, *et al,* Nucl. Fusion **41** (2001) 1423.

[18] M P Gryaznevich and S E Sharapov, Plasma Phys. Control. Fusion **46** (2004) s15.

[19] S D Pinches, H L Berk, M P Grayaznevich, S E Sharapov, and JET-EFDA Contributors, Plasma Phys. Control. Fusion **46** (2004) S47.

[20] M R Tournianski, R J Akers, P G Carolan, D L Keeling, Plasma Phys. Control Fusion **47** (2005) 671.

[21] S.E. Sharapov, B. Alper, F. Andersson, Yu. F. Baranov, H.L. Berk, L. Bertalot, D. Borba, C. Boswell, B.N. Breizman3, R. Buttery, C.D. Challis, M. de Baar7 . de Vries, L.-G. Eriksson, A. Fasoli, R. Galvao, V. Goloborod'ko, M.P. Gryaznevich, R.J. Hastie, N.C. Hawkes, P. Helander, V.G. Kiptily, G.J. Kramer, P.J. Lomas, J. Mailloux, M.J. Mantsinen, R. Martin, F. Nabais, M.F. Nave, R. Nazikian, J.-M. Noterdaeme, M.S. Pekker, S.D. Pinches, T. Pinfold, S.V. Popovichev1 , P. Sandquist, D. Stork, D. Testa, A. Tuccillo, I. Voitsekhovich, V. Yavorskij, N.P. Young, F. Zonca, JET-EFDA Contributorsa and the MAST Team, Nucl. Fusion **45** (2005) 1168–1177.

[22] M.P. Gryaznevich, S.E. Sharapov, M. Lilley, S.D. Pinches, A.R. Field, D. Howell, D. Keeling, R. Martin, H. Meyer, H. Smith, R. Vann, P. Denner, E. Verwichte and the MAST Team, Nucl. Fusion **48** (2008) 084003.

[23] K G McClements, M P Gryaznevich, S E Sharapov, R J Akers, L C Appel, G F Counsel, C M Roach, R Majeski, Plasma Phys. Contol. Fusion **41** (1999) 661.

[24] M P Gryaznevich and S E Sharapov, Nuclear Fusion **40** (2000) 907.

[25] L. Chen, Phys. Plasmas **1** 1519 (1994).

[26] C Z Cheng, N N Gorelenkov, and C T Hsu, Nucl. Fusion **35**, 1639 (1995).

[27] Y Todo, K Shinohara, M Takechi, M Ishikawa, J. Plasma Fusion Res. **79** (2003) 1107.

[28] E D Fredrickson, L Chen, R B White, Nucl. Fusion **43** (2003) 1258.

[29] N N Gorelenkov, H L Berk, E Fredrickson, S E Sharapov, Proceedings for the 34th European Physical Society Conference on Plasma Physics, Warsaw, Poland June 2-6, 2007, paper I3.006.

[30] N. N. Gorelenkov, M. A. Van Zeeland, H. L. Berk, N. A. Crocker, D. Darrow, E. Fredrickson, G.-Y. Fu, W. W. Heidbrink, J. Menard, and R. Nazikian, Phys. Plasmas **16** 056107 (2009).

[31] D. Yu. Eremin and A. Könies, Phys. of Plasmas **17**, 0012108 (2010).

[32] N.N. Gorelenkov, C.Z. Cheng, Nucl. Fusion 35, (1995) 1743.

[33] N.N. Gorelenkov, C.Z. Cheng, Phys. Plasmas 2 (1995) 1961.

[34] N N Gorelenkov, C Z Cheng, E Fredrickson, Phys. Plasmas 9 (2002) 3483.

[35] N N Gorelenkov, C Z Cheng, E Fredrickson, E Belova, D Gates, S Kaye, G J Kramer, R Nazikian, R B White, Nucl. Fusion 42 (2002) 977.

[36] N.N. Gorelenkov, E. Fredrickson, E. Belova, C.Z. Cheng, D. Gates, S. Kaye, and R. White, Nucl. Fusion, 43 (2003) 228.

[37] E Belova, N N Gorelenkov, C Z Cheng, E D Fredrickson, in Proceedings of the 30th European Physical Society Conference on Controlled Fusion and Plasma Physics, St. Petersburg, Russia, July 2003, ECA Vol. 27A, P-3.102.

[38] V. S. Belikov and Ya. I. Kolesnichenko, R. B. White, Phys. of Plasmas 10 (2003) 4771.

[39] Eliezer Hameiri, Akihiro Ishizawa and Akio Ishida, Phys. Plasmas **12**, 072109 (13pages) (2005)

[40] W W Heidbrink, E D Fredrickson, N N Gorelenkov, T L Rhodes, M A Van Zeeland, Nucl. Fusion **46** (2006) 324.

[41] Ya. Kolesnichenko, R B White, Yu. V Yakovenko, Phys.of Plasmas 13 (2006) 122503,

[42] E.V. Belova, S. C. Jardin, H. Ji, M. Yamada, and R. Kulsrud, Phys. Plasmas **7** (2000) 4996

[43] *Numerical Modeling of NBI-Driven Sub-Cyclotron Frequency Modes in NSTX*, E. Belova *in Bulletin of the American Physical Society, 52nd Annual Meeting of the Division of Plasma Physics, Nov. 8-12, 2010, Chicago, IL* paper TI2-3, *to be published in Phys. of Plasmas*.

[44] L C Appel, T Fülöp, M J Hole, H M Smith, S D Pinches, R G L Vann and The MAST Team, Plasma Phys. Control. Fusion **50** (2008) 115011.

[45] H. L. Berk, B. N. Breizman, M. Pekker, Phys. Plasmas **2**, 3007 (1995)

[46] H. L. Berk, B. N. Breizman, M. Pekker, Nucl. Fusion, **35**, (1995) 1713.

[47] H.L. Berk, B. N. Breizman, J. Fitzpatrick, H. V. Wong, Nucl. Fusion **35** (1995) 1661.

[48] D. Stutman, L. Delgado-Aparicio, N. Gorelenkov, M. Finkenthal, E. Fredrickson, S. Kaye, E. Mazzucato, and K. Tritz, Phys. Rev. Lett. **102**, 115002 (2009).

[49] Ya. I. Kolesnichenko, Yu. V. Yakovenko, and V. V. Lutsenko, Phys. Rev. Lett. **104** (2010), 075001.

[50] N.J. Fisch, J-R. Rax, Phys. Rev. Lett. **69** (1992) 612.

[51] M C Herrmann and N Fisch, Phys. Rev. Lett. **79** (1997) 1495.

[52] N. J. Fisch, A. Fruchtman, C. F. F. Karney, M. C. Herrmann, and E. J. Valeo, Phys. Plasmas **6**, 2375 (1995).

[53] N N Gorelenkov, N J Fisch and E Fredrickson, Plasma Phys. Control. Fusion **52** (2010) 055014.

[54] G R Smith, A N Kaufman, Phys. Rev. Lett. **34** (1975) 1613.

[55] C F F Karney, A Bers, Phys. Rev. Lett. **39** (1977) 550.

[56] C F F Karney, Phys. Fluids **21** (1978) 1584.

[57] J Y Hsu, K Matsuda, M S Chu, T H Jensen, Phys. Rev. Lett. **43** (1979) 203.

[58] J. F. Drake, T. T. Lee, Phys. Fluids **24** (1981) 1115.

[59] L Chen, Z Lin, R White, Phys. Plasmas **8** (2001) 4713.

[60] J M McChesney, R A Stern, P M Bellan, Phys. Rev. Lett. **59** (1987) 1436.

[61] J M McChesney, P M Bellan, R A Stern, Phys. Fluids B **3** (1991) 3363.

[62] A D Bailey III, P M Bellan, R A Stern, Phys. Plasmas **2** (1995) 2963.

[63] A D Bailey III, R A Stern, and P M Bellan, Phys. Rev. Lett. **71** (1993) 3123.

[64] S J Sanders, P M Bellan, R A Stern, Phys. Plasmas **5** (1998) 716.

[65] E D Fredrickson, C K Phillips, J Hosea, J R Wilson, P Bonoli, N N Gorelenkov, J Wright, E Valeo, *in Radio Frequency Power in Plasmas, 17th Topical Conference on Radio Frequency Power in Plasmas, Clearwater, Florida, 7-9 May 2007*, AIP Conference Proceedings, Vol. 933, Eds. P M Ryan, D A Rasmussen, Melville, New York, 2007, p111.

[66] S Kubota, X V Nguyen, W A Peebles, L Zeng, E J Doyle, Rev. Sci, Instrum. **72** (2001) 348.

[67] D. R. Smith, H. Feder, R. Feder, R. J. Fonck, G. Labik, G. R. McKee, N. Schoenbeck, B. C. Stratton, I. Uzun-Kaymak, and G. Winz, Rev. Sci. Instrum. **81** 10D717(2010).

[68] K. Tritz, D. Stutman, M. Finkenthal (JHU) R. Bell, E. Belova, E. Fredrickson, N. Gorelenkov, R. Kaita, S. Kaye, B. LeBlanc, E. Mazzucato, Y. Ren, R. White, N. Crocker, S. Kubota, W.A. Peebles, R. Fonck, G. McKee, D.R. Smith, and the NSTX Team, *in Bulletin of the American Physical Society, 52nd Annual Meeting of the Division of Plasma Physics, Nov. 8-12, 2010, Chicago, IL* paper PI2-2, p238, *to be published in Phys. of Plasmas*.

[69] I.T. Chapman, M.-D. Hua, S.D. Pinches, R.J. Akers, A.R. Field, J.P. Graves, R.J. Hastie, C.A. Michael and the MAST Team, *Nucl Fusion* 50 (2010) 045007

[70] M. Podestà, W. W. Heidbrink, R. E. Bell, and R. Feder, Rev. Sci. Instrum. **79**, 10E521 (2008).

[71] D.S. Darrow, Rev. Sci. Instrum. **79**, 023502 (2008)

[72] N. A. Crocker,W. A. Peebles, S. Kubota, E. D. Fredrickson, S. M. Kaye, B. P. LeBlanc, J. E. Menard, Phys. Rev. Lett. **97** (2006) 045002.

[73] E. D. Fredrickson, N. Gorelenkov, E. Belova, N. A. Crocker, S. Kubota, B. LeBlanc, R. E. Bell, D. R. Smith, M. Podesta, H. Yuh, F. Levinton, in proceedings of the 23rd IAEA Fusion Energy Conference, 11 - 16 October 2010, Daejeon, Korea, (IAEA, Vienna, 2011) paper IAEA-EXW/P7-06

[74] G. J. Kramer, R. B. White, R. Nazikian, and H. L. Berk, *Fusion-born Alpha Particle Ripple Loss Studies in ITER,* in proceedings of the 22nd IAEA Fusion Energy Conference, 13-18 October 2008, Geneva, Switzerland, (IAEA, Vienna, 2012) paper IAEA-IT/P6-3.

[75] D. A. Gates, N. N. Gorelenkov, and R. B. White, Phys. Rev. Lett. **87** 205003 (2001).

The Princeton Plasma Physics Laboratory is operated
by Princeton University under contract
with the U.S. Department of Energy.

Information Services
Princeton Plasma Physics Laboratory
P.O. Box 451
Princeton, NJ 08543

Phone: 609-243-2245
Fax: 609-243-2751
e-mail: pppl_info@pppl.gov
Internet Address: http://www.pppl.gov